Journal of the European Ceramic Society 20 (2000) 537–544

Chemical vapor deposition of ZrO_2 and C/ZrO_2 on mullite fibers for interfaces in mullite/aluminosilicate fiber-reinforced composites

K. Nubian[b], B. Saruhan[a,*], B. Kanka[a], M. Schmücker[a], H. Schneider[a], G. Wahl[b]

[a]*German Aerospace Center, Institute for Materials Research, 51147 Köln, Germany*
[b]*University of Braunschweig, Institute for Surface Technology, 38108 Braunschweig, Germany*

Accepted 10 August 1999

Abstract

For the realization of crack deflection and fiber pull-out in aluminosilicate fiber-reinforced dense mullite-matrix composites, suitable fiber/matrix-interfaces are an important requirement in order to obtain sufficiently weak bondings between fibers and matrices. Two types of chemical vapor deposited (CVD) fiber/matrix-interfaces have been studied in the present work porous ZrO_2 and C/ZrO_2-double layers. In the latter case, carbon was burned out to form a gap during the processing of composites (fugitive coating). Porous ZrO_2 coatings were produced by an optimized CVD-process with Zr-acetylacetonate as a precursor. The constancy of the layer thickness depended on the deposition temperature. It was found that at a temperature of approximately 300°C and a pressure of 5 hPa, suitably uniform layers with thickness ranging between 100 and 300 nm were achieved. The coatings contained approximately 15 wt% carbon which produced, after annealing in air, a porous structure. The deposition kinetics can be described by a first order reaction. The carbon layer in C/ZrO_2-double layers was produced by using propane. The thickness of carbon layer was 10 and 100 nm, respectively. Aluminosilicate fiber/mullite matrix composite prepegs were fabricated by infiltration of coated and unidirectionally oriented fiber (0°) with a slurry, containing a pre-mullite powder, calcined at 1100°C. Uniaxial hot-pressing of dried prepegs was carried out at <1250°C for 15 min, at 20 MPa. Prepegs with ZrO_2 fiber/matrix-interfaces were hot-pressed in air, while the samples with C/ZrO_2-interfaces were processed in flowing argon. After hot-pressing, samples with C/ZrO_2-interfaces were heat-treated in air (1000°C) in order to burn out the C-layer (fugitive coating). These composites yielded a controlled fracture with a high deflection rate and a favorable fracture strength of about 200 MPa, due to crack-deflection and fiber pull-out. Composites with ZrO_2-interfaces, on the contrary yielded no crack deflection or pull-out. Therefore, they are less damage tolerant than those having C/ZrO_2 double layer systems. © 2000 Elsevier Science Ltd. All rights reserved.

Keywords: Aluminosilicate fibres; Composites; Interfaces; Mullite matrix; ZRO_2

1. Introduction

Thermal protection systems consisting of oxide-based fiber-reinforced composites can contribute significantly in the reduction of NO_x and emission in the combustion chambers of aircraft engines and stationary gas turbine engines. Relying on good thermal properties of the ceramics, less cooling, thus, less fuel consumption will be necessary. Nevertheless, strong bonding at the fiber/matrix-interfaces due to the chemical and mechanical interactions causes brittleness of ceramic composites, making them less damage tolerant and, therefore, less reliable for the application.

For achievement of advantageous failure in the composites, one approach is to apply porous interphases, thus lowering the shear strength and constituting a preferred path for the diversion of matrix-originating cracks. An example of this approach is given by Si–O–N coating on SiC-fibers.[1] The required porosity was generated with latex polystyrene mixed with Si_3N_4 and SiO_2-powders. Push-out tests showed that only those coatings which were retreated with a silica layer displayed a reasonably low (25 MPa) friction-stress at room temperature. Another method, describing a successful pseudo porous fiber coating system by means of CVD, used a 0.5–50 μm thick layer of carbon-enriched SiC-coating.[2] The carbon source was methane, and the SiC source was either methyltrichlorosilane or tetrachloride. After heat-treatment at a temperature range between 800 and 1200°C under reduced pressure (1–100 Torr), crystalline SiC with a resulting porosity of 12% was obtained.

The only effective way in coating of fiber surfaces in fiber tows or fabrics with thin ceramic layers is to

* Corresponding author. Tel.: +49-2203-601-3228; fax: +49-2203-696480.
E-mail address: bilge.saruhan@dlr.de (B. Saruhan).

0955-2219/99/$ - see front matter © 2000 Elsevier Science Ltd. All rights reserved.
PII: S0955-2219(99)00251-4

employ processes which have a large throwing power. The CVD process is one of such processes. Deposition of SiC or BN coatings on fibers with CVD process has been proven to be successful.[3] This paper describes methods for coating of Nextel™ 720-mullite/alumina-fibers with a porous ZrO_2-layer and with a C/ZrO_2-double layer resulting in a fugitive coating, sealed with a porous oxide layer.

2. Experimental

2.1. Materials

Precursors with high vapor pressures at moderate temperatures are preferred for CVD-coatings. Candidate precursors are chlorides, alkoxides and β-dikatonates. Zirconium acetylacetonate [$Zr(acac)_4$] is a β-dikatonate and has a vapor pressure of approx. 700 Pa at 200°C, which is high enough to be used in CVD-processes. The CVD processing of $Zr(acac)_4$ to produce ZrO_2-coatings on flat substrates was described in the literature.[4–7] These studies reported that some carbon was entrapped in the coating system, because of the incomplete decomposition on the substrate surface. This characteristic of the precursor may be benefited for the synthesis of porous ZrO_2-layers, without application of another substance for achievement of porosity. The $Zr(acac)_4$ powder was of 98% purity and provided by FLUKA (Germany).

The woven fiber fabrics (8 harness Atlas) were of mullite/alumina [Nextel(720)] and were provided by 3M (Minnesota, USA). The fabrics had the form shown in Fig. 1. Woven fiber tows were consisted of fibers with a diameter of 12 μm. The chemical composition was 85 wt% Al_2O_3 and 15 wt% SiO_2 with a density of 3.4 g/cm^3. Each fiber tow contains approximately 400 single fibers.

The matrix material for the composites was produced by hot-pressing pre-mullite powders (Siral, CONDEA, Germany). This powder has a purity of 99.99% and is amorphous in the as-received form.

2.2. CVD-process and experimental equipment

Decomposition temperature of $Zr(acac)_4$ is rather low, hence evaporation rate becomes unstable, if it is heated for longer times at temperatures above 160°C.[4] This behavior requires special evaporation equipment, which is shown schematically in Fig. 2. The powdery precursor is transported through a rotating plate with holes into the evaporator which is heated to 200°C and there evaporates spontaneously. The carrier gas with the precursor then is transported through tubes to the furnace. The precursor concentration in the gas was adjusted to 0.1 mol% at a gas flow of 200 sccm argon. All piping was made of stainless steel and heated to 500 K. Typical deposition conditions were: deposition temperature 300–500°C, pressure 500 Pa.[4]

The deposition equipment is shown in Fig. 3. In this equipment, two different evaporators were installed, in order to produce multi-component coatings if necessary. The reaction gas was transported into a quartz tube in a resistance heated furnace. The internal diameter of the quartz tube was 10.5 cm and the aluminosilicate fiber fabrics, cut into rectangles of 50×50 mm^2, were installed in this quartz tube. The fabrics were arranged at a position perpendicular to the gas flow. Maximum 4 samples could be placed in the resistance furnace. The deposited quantity was measured by the mass difference before (m_1) and after the deposition (m_2) $\Delta m = m_2 - m_1$. The molar deposition rate was calculated by assuming that ZrO_2 is deposited:

$$\dot{n}_m = \frac{\Delta m}{AM} \tag{1}$$

where M is the molar mass of ZrO_2.

The carbon precoating of the Nextel fibers was carried out under a pressure of 12 hPa at a deposition temperature of 950°C for 45 min. The carrier gas was propane and its flow rate was set to 167 sccm.

2.3. Processing of composites

The pre-mullite (Siral) powder was calcined at about 1100°C prior to preparation of the slurry. X-ray diffraction data of this calcined powder yielded a weakly crystalline γ-Al_2O_3 phase, accompanied by some SiO_2-rich amorphous phase. Formation of mullite under given hot-pressing conditions occurred after 1 minute holding time at 1250°C. Just at the hot-pressing temperature, without any holding time, no mullite formation was observed. For a full transformation to mullite, it was necessary to hold for 15 min at 1250°C under 20 MPa. Prolonged holding times yielded no improvement in the densification and mullitization. In order to avoid fiber damage, the optimum holding time was limited to 15 min.

Slurry was prepared by mixing of the calcined powders with binder and disperser in an aqueous media. Although, for coating, the fiber fabrics were used, for the preparation of the prepegs, the fiber tows were pulled out of the fabric to fabricate 1D-unidirectional fiber composites. As-coated fiber tows were immersed in the slurry and formed to rectangular shaped plates on plaster of Paris moulds. After drying the prepegs in air, the stacked prepegs were uniaxially cold-pressed under approximately 2 MPa pressure. Hot-pressing of the ZrO_2-coated fiber composites was carried out in air at 1250°C for 15 min under 20 MPa uniaxial pressure. C/ZrO_2-coated fiber composites were also hot-pressed under the same conditions, however in flowing argon

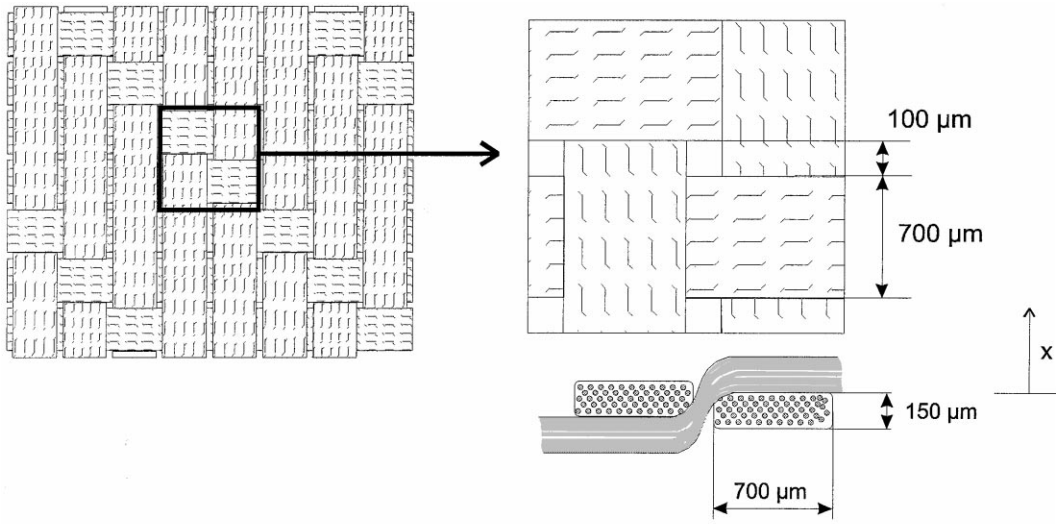

composition	Al_2O_3	85 wt.%
	SiO_2	15 wt.%
crystalline phases		alpha alumina + mullite
filament diameter		12 µm
filament density		3.4 g/cm³
number of filaments / bundle		400
porosity of a bundle		0,57
specific surface of bundle		$9{,}8 \cdot 10^2$ cm²/g
substrate size		50 mm x 50 mm

Fig. 1. Schematic view of the Nextel 720 fiber fabric.

which was introduced into the system above about 400°C [Fig. 4(a) and (b)]. For both cases, the pressure was applied at about 1100°C, as soon as the first shrinkage occurs. Hot-pressing was carried out mould-free between SiC-punches in order to achieve a homogeneous temperature distribution on the sample plate.

2.4. Characterization of composites

Phase analysis of the matrix and the coating were carried out by X-ray powder diffraction at room temperature (SIEMENS, D5000, Germany) using Ni-filtered CuK_α radiation. Diffraction patterns were recorded in step scan mode (3s/0.05, 2θ) in the 10–80° 2θ range. Microstructural investigations were carried out with optical and electron microscopy studies were done with LEO field emission scanning electron microscopy and with PHILLIPS EM 430 transmission electron microscopy (TEM), 300 kV accelerating voltage. Sample preparation performed by dimple grinding and subsequent ion beam milling. Samples were coated with carbon to avoid charging effect.

3. Results and discussion

3.1. Deposition of ZrO_2

Fig. 5 shows the measured deposition rate on the fabric and on the Al_2O_3 wafer vs the reciprocal absolute temperature. The temperature dependence of the deposition rate can be described by an Arrhenius plot

$$\dot{n}_m \sim \exp(-\frac{E}{RT}) T < 370°C \quad (2)$$

Thus, the activation energy $E = 24 + -3$ kJ/mol of ZrO_2 deposition on the fabric was calculated. The calculated activation energy E for the fiber fabric is much smaller than the values given in literature for ZrO_2-deposition on flat substrates ($E = 80 + -7$ kJ/mol). [4] A plane Al_2O_3-wafer was coated as a reference under the same conditions. The activation energy was $E = 66 + -5$ kJ/mol which is in good accordance with literature.[4] The deposition rate related to the fiber surface on the fabric is much lower than on the Al_2O_3-wafer. This is

because the deposition rate on the fibers is not only determined by the chemical reaction, but also by the diffusion of the reactive gas into the fiber bundle. The deposition conditions are given above. At temperatures $T > 370°C$ the deposition rate of ZrO_2 decreases according to Fig. 5 because of strong powder formation in the gas phase which was observed on all walls.

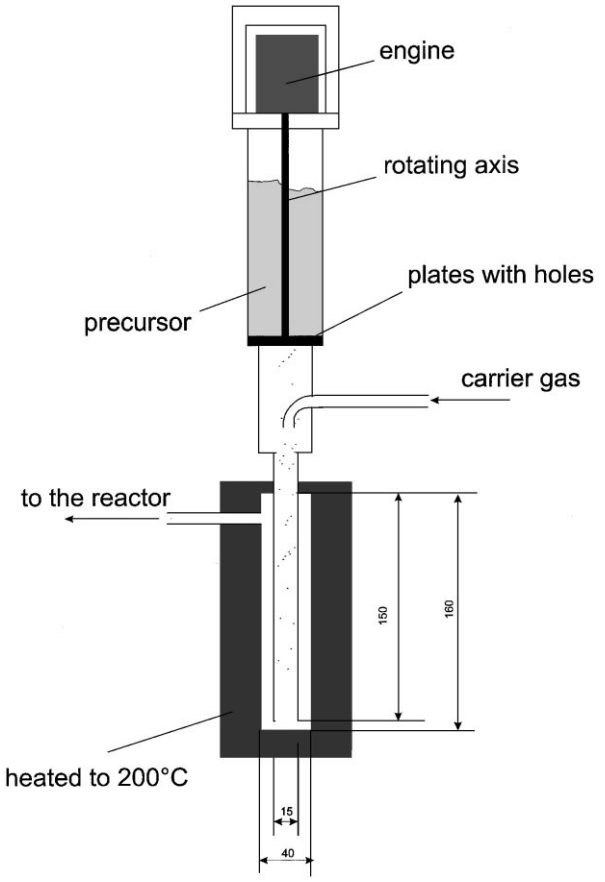

Fig. 2. Evaporation equipment used for CVD-coating experiments.

The scanning electron microscopy observations of the fibers coated at 310 and 370°C demonstrates that the coatings deposited at 310°C were more uniform and complete than those deposited at 370°C. The surface of the ZrO_2-coating, obtained at 310°C were smooth and between the fibers, no pasting was observed. The 370°C, deposited coating surfaces were rough and incomplete. Only a few fibers were coated, while most fibers were free of any coating.

In order to determine the distribution of the layer thickness on the single fibers inside the fabric, one fiber

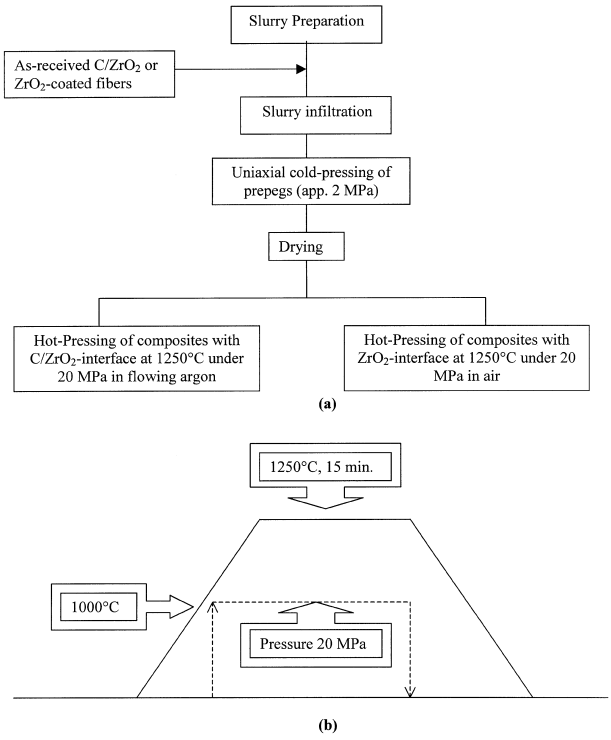

Fig. 4. (a) Flow chart showing the details in fabrication of composites and (b) schematic presentation of the hot-pressing process during fabrication of composites.

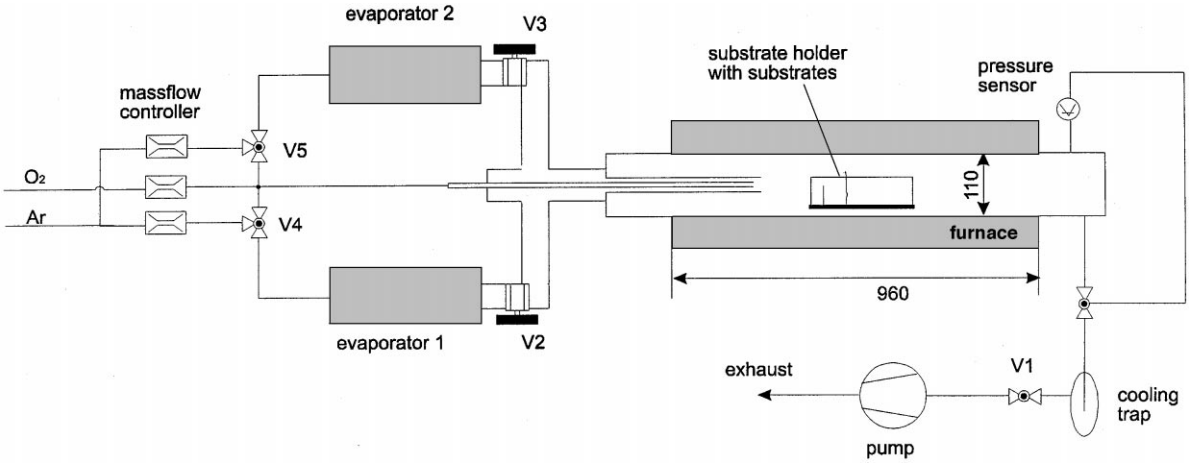

Fig. 3. Schematic drawing of the CVD-equipment.

bundle was removed from the fabric and embedded in resin (G-1 Epoxy, GATAN Inc.). After breaking the embedded bundle the thickness of the coatings on the single fibers could be measured by SEM. In each sample approx. 80 single fibers taken at random in the bundle were measured. The resulting thickness distributions are shown in Fig. 6. It shows that the thickness on the fibers is more constant at lower temperatures. This can be expected because the depletion in the gas phase decreases with the temperature. The thickness distribution can be explained by Fick's law for the diffusion in a porous medium if a first order reaction for the ZrO_2 deposition is assumed.[8]

$$j = -\frac{\varepsilon}{q} D \frac{\mathrm{d}c}{\mathrm{d}x} \tag{3}$$

ε is the porosity of the fiber bundle produced by the fibers, D is the gas diffusion coefficient of the precursor in the carrier gas, c is the molar concentration of the precursor in the gas phase, q is the tortuosity, j is the current diffusion density related to the cross-section of

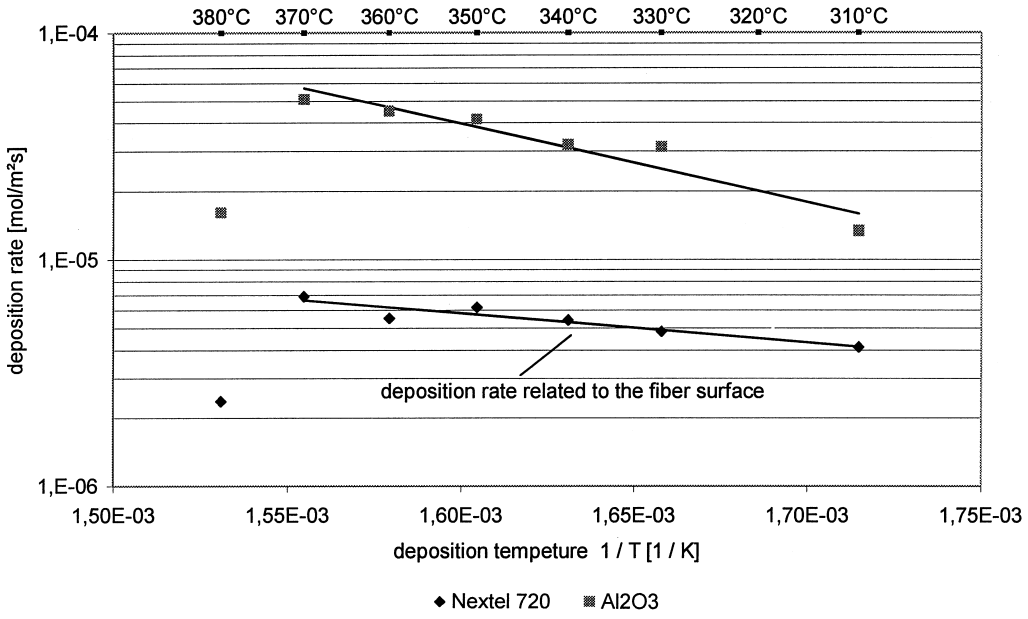

Fig. 5. Deposition rate of ZrO_2 from $Zr(acac)_4$ vs reciprocal deposition temperature on the Nextel 720 fiber fabric and on Al_2O_3-wafer ($P = 500$ Pa, flow = 200 sccm argon).

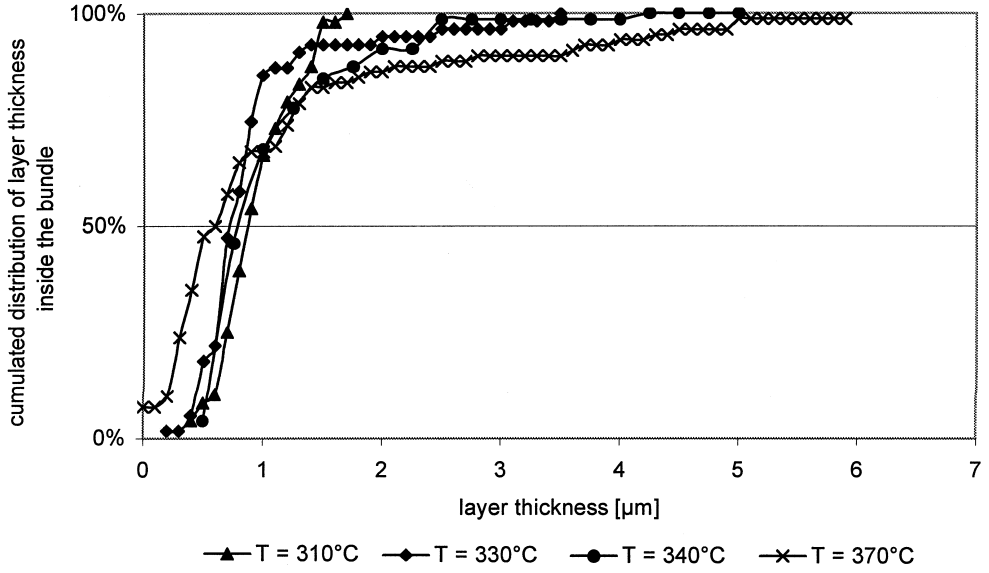

Fig. 6. Cumulated distribution of layer thickness in a single fiber bundle (80 fibers measured for each bundle).

the porous medium, x is the distance to bundle surface. In order to improve the constancy of the layer thickness according to Fig. 6 the deposition temperature should be as low as possible. Experiments show, however, that no deposition is possible at temperatures below 300°C because the reaction velocity is too slow. So deposition temperatures at about 310°C was found optimum.

X-ray diffraction data of the fibers CVD-coated at 370°C showed that the coatings just after the CVD-process were amorphous ZrO_2. After a heat-treatment at 1250°C or during hot-pressing of composites at 1250°C, the coatings were converted to monoclinic ZrO_2. On determination of mass changes of the coated fibers after heat-treatment at 700°C in oxygen, a weight loss of approximately 15 wt% was found, indicating the presence of residual carbon in the as-coated form, due to the incomplete decomposition of the $Zr(acac)_4$. This value is in good agreement with the literature data of Brennfleck et al. [6]

3.2. ZrO_2 and C/ZrO_2-interfaces in mullite/aluminosilicate fiber-reinforced composites ZrO_2-interfaces

Transmission electron microscopic investigations of the composites with ZrO_2 fiber/matrix-interface yielded porous ZrO_2 layers with a thickness of about 200–500 nm (Fig. 7). In a first approach, we assumed that pore formation was mainly caused by burn-out process of the residual carbon which was in the order of 15%. More detailed inspection of the microstructure in ZrO_2-layer showed that the porous ZrO_2 after hot-pressing can not be due only to burn-out. This was derived from the observation that the interphase displays an open porosity which is homogeneously distributed between well-rounded and isolated ZrO_2 grains (Fig. 7). Furthermore, the pores do not present the open channel-type pore formation typical for volatilization processes. Therefore, we believe that crystallization processes as well as burn-out can be held responsible.

In spite of their relatively high interface porosity, the composites with ZrO_2 fiber/matrix-interfaces show no fiber pull-out [Fig. 8(a)] and display stress–strain curves corresponding to brittle fracture behavior. Scanning electron microscopy investigations on the fracture surfaces reveal that the fiber/matrix bonding, despite the presence of a porous ZrO_2 layer, was strong. Especially in hot-pressing direction, the matrix at the contact points to the fibers is highly densified and is in intense contact to the interfaces. The area around the fibers, perpendicular to the hot-pressing direction on the contrary are less den-

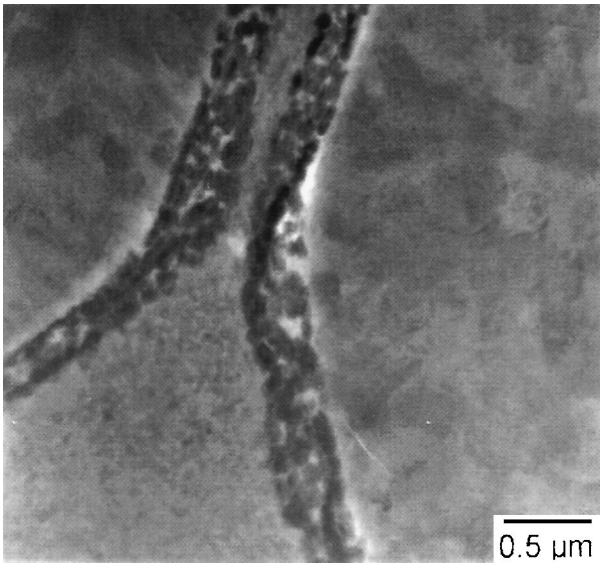

Fig. 7. Transmission electron microscopic image of ZrO_2 fiber/matrix interfaces in mullite matrix composite. The interfaces consist of porous ZrO_2 layers with a thickness of about 500 nm.

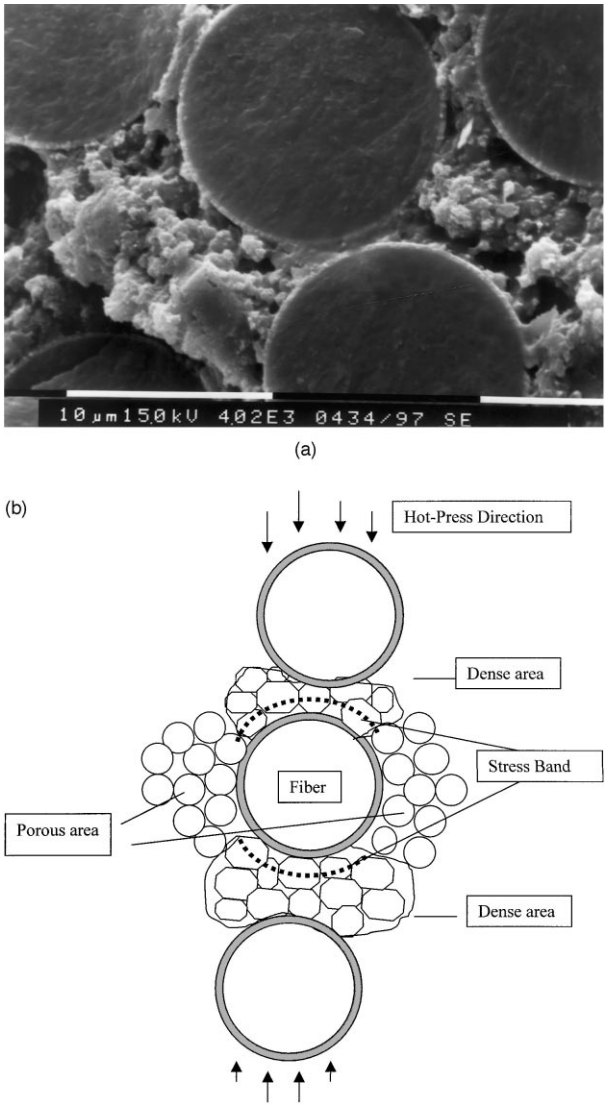

Fig. 8. (a) Scanning electron microscopic image and (b) schematic drawing of interfacial conditions after hot-pressing in unidirectionally aluminosilicate fiber-reinforced/porous ZrO_2 interphase and mullite matrix composites.

sified and the porous matrix is only partly in contact to the fiber interfaces. Obviously, there exist radial stress gradients around the fibers with high stress concentration in hot-pressing direction [Fig. 8(b)]. We believe that the processing conditions (e.g. phase combination of the matrix material, temperature and the way how the pressure was applied, phase transformation occurring in the matrix and the interphase material, etc.) may have great influence on the possible formation of strong bonding at the interface. The slurry infiltrated pre-composite contains as a matrix amorphous SiO_2-rich phase which softens at relatively lower temperatures. During hot-pressing, the amorphous phase in the matrix facilitates sintering, versus a viscous flow of γ-Al_2O_3-particles before transforming to mullite at 1250°C. The sintering experiments show that mullite formation does occur at temperatures $\geqslant$1250°C only. This means that the amorphous phase is present throughout the whole processing line and may lead to strong bonding with the interface.

3.3. C/ZrO_2-interfaces

A further approach in order to achieve damage tolerant composites, weakening of fiber/matrix-bonding and elimination of the process-related stresses between fibers and matrix has been established by using the fugitive coating concept. These fiber/matrix-interfaces consist of C/ZrO_2 double layers and are deposited by CVD. Since hot-pressing was performed in argon atmosphere, the carbon layer acted as a buffer zone and that way prevented exaggerated interfacial fiber/matrix bonding and also the formation of compressive stresses at the matrix/fiber-interfaces in hot-pressing direction. TEM investigations on as-hot-pressed samples confirmed the existence of thin (10–100 nm) amorphous carbon layers surrounding fibers. After burn-out of the carbon layers in air thin gaps between fiber and ZrO_2-layer are formed [Fig. 9(a)]. Scanning electron microscopy observations and stress–strain curves of the C/ZrO_2-interface composites demonstrate that an extensive fiber pull-out, thus damage tolerant behavior is achieved [Fig. 9(b)]. Crack deflection occurs at the gap, while the ZrO_2-layer remains attached to the matrix. Apparently, the thickness of the fugitive coating plays a major role for the damage tolerant behavior of the composite. A broad gap surrounding the fiber can not work, since the required load-transfer between matrix and fibers does not occur. On the other hand, if the gap is too narrow, many local contact points between the matrix and fiber develop, leading to a strong fiber/matrix bonding and an associated brittle fracture behavior of the composite. Our present studies have shown that carbon layers with thickness ranging between about 10 and 100 nm are suitable for fugitive coatings. Obviously the ideal gap thickness is that which enables the fiber to remain uncompressed, at the same time, allows energy dissipating crack deflection process to take place. Therefore, the gap thickness should be at the same order as surface roughness of fiber and matrix.

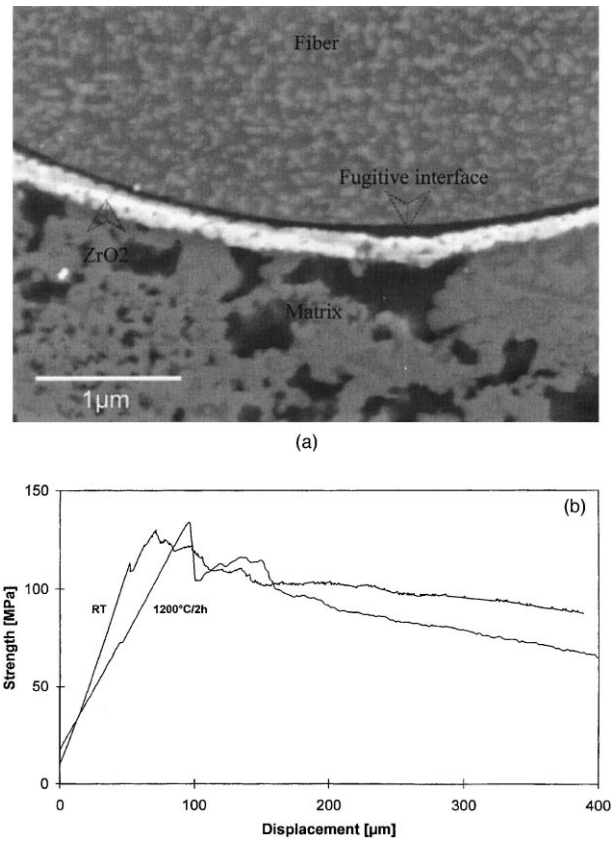

Fig. 9. Scanning electron image of interface in C/ZrO_2-coated mullite fiber mullite matrix composites (a) and 3-point-bending stress-strain curve of this composite.

4. Conclusions

The ZrO_2 deposition was described by a first order reaction. Deposition temperatures about 300°C was found to be optimum for ZrO_2-coating on fiber fabrics, compared to higher temperatures used with dense wafers. Use of Zr-acetylacetonate resulted in porous coatings after hot-pressing the oxided/oxide fiber-reinforced composites. C/ZrO_2-double coating are achieved by successive CVD-coating with propane and Zr-acetylacetonate.

Composites are fabricated by infiltration of coated fiber yarns with pre-mullite slurry and consequently hot-pressing the infiltrated prepegs. Porous ZrO_2-coating at interface of mullite/aluminosilicate fiber-reinforced composites displayed no fiber-pull-out. C/ZrO_2, in turn, resulted in damage tolerant fracture of the composites. The mechanical and microstructural observations of the composites at RT and at 1200°C after 2 h heat-treatment showed that a thickness of 10 nm for the

gap was insufficient for providing an effective long-term damage-tolerance. While a gap thickness of 100 nm can be regarded as maximum, thus gap ranging between 50 and 100 nm can be recommended for successful results.

Acknowledgements

Ms. Gudrun Paul is thanked for her careful work in preparation of the difficult TEM samples of the composites.

References

1. Ogbuki, L. U. J. T., A porous oxidation-resistant fiber coating for CMC interphase. *Ceram. Eng. Sci. Proc.*, 1995, **6**(4), 497–505.
2. Scheffier, W., Multilayer fiber coating, US Patent No. 5,445,106, 1996.
3. Stolle, R. and Wahl, G., Direct transfer of kinetic data from a microbalance equipment into a tube reactor for CVD-BN on SiC fabrics. *Advanced Materials, Chem. Vap. Deposition*, 2000, in press.
4. Pulver, M. and Wahl, G. *Proc. of the 14th Int. Conf. and 11th European Conf. on CVD*, l997, 960–967.
5. Fukuda, R., Nagata, S., Negishi, A., Kasuga, Y., and Okuo. T., Comm. Eur. Communities, Report, 1991.
6. Brennfleck, K., Fitzer, E. and Schoch, G., In *Proc. of 5th Europ. Conf. CVD*, ed. J. O. Carlsson and J. Lindström, Uppsala, 1985, pp. 63–70.
7. Balog, M., Schieber, M., Michman, M. and Patai, S., *Thin Solid Films*, 1977, **47**, 109–120.
8. Carman, P. C., *Flow of Gases through Porous Media*. Butterworths Scientific Publications, London, 1956.